

FATIGUE CRACK CLOSURE WITH NEGATIVE STRESS RATIO FOLLOWING
SINGLE TENSILE OVERLOADS IN 2024-T3 and 7075-T6 ALUMINUM

D. P. Musil and R. I. Stephens*

INTRODUCTION

A great deal of research on crack closure has occurred following Elber's first introduction of the crack closure model [1]. Most experimental programmes, however, have dealt only with positive stress ratio cyclic loading for both constant amplitude and spectrum loading. Unfortunately, complete tensile load sequences do not constitute the majority of loading spectra. Characterization of fatigue crack growth behaviour has indicated that both large and small cyclic compressive stresses following single tensile overloads can drastically reduce fatigue crack retardation (delay) in both low and high strength materials [2 - 6]. The compression portion of the load cycle following single tensile overloads has substantially greater influence than that found from just constant amplitude cycling. Thus the compression portion of a load spectrum should not be neglected in crack growth calculations.

The above mentioned research [2 - 6] has only served to characterize the effects of compressive stresses following single tensile overloads and has made no attempt to explain or correlate the observed results with crack closure measurements. The objectives of this research were outlined in hopes of determining if differences in delay with $R = 0$ and $R = -1$ following single tensile overloads could be explained using the crack closure model. Crack closure measurements were made at various crack lengths following a single tensile overload and correlated with the observed delay.

TEST PROCEDURES

The materials used in this investigation were 2024-T3 and 7075-T6 aluminum which were from the same plate used in previous studies [2 - 4]. Single edge notch specimens shown in Figure 1 with two thicknesses of 3.15 mm and 0.3 mm were used. Specimens were fatigue pre-cracked to an initial crack length $a_0 = 6.35$ mm where both constant amplitude reference tests and single tensile overload tests were begun. Fatigue tests were performed at room temperature in a closed-loop electrohydraulic test system under load control conditions. Loads were transmitted through a spherical monoball gripping system to ensure axial loading in both tension and compression. Constant amplitude loading for both $R = 0$ and $R = -1$ was at 15 Hz while tensile overloads were applied at 0.02 Hz. Crack lengths were measured using a 36x optical microscope with stroboscopic lighting and a least division photo-etch longitudinal grid system of 0.25 mm. The initial maximum stress intensity with $a_0 = 6.35$ mm was $12.3 \text{ MPa}\sqrt{\text{m}}$. All overload ratios, $\text{OLR} = P_{\text{O}}/P_{\text{max}}$ as shown inserted in Figure 3, were 2.25

*Research Assistant and Professor, respectively, Materials Engineering Division, The University of Iowa, Iowa City, Iowa, U.S.A.

which resulted in overload stress intensities of $27.7 \text{ MPa}\sqrt{\text{m}}$. Following the single tensile overload, specimens were cycled to fracture with $R = 0$ or $R = -1$. Nine specimens were tested with 2024-T3 and eight with 7075-T6 which included constant amplitude reference tests with $R = 0$ and -1 for both thicknesses and a single overload test for each thickness and R ratio. Two duplicate tests were obtained.

Crack closure measurements were obtained from a surface CTOD gage pin-mounted 2.5 mm behind the crack tip front. The CTOD gage consisted of four 350 ohm foil gages bonded to a working beam. A special gage mounting apparatus was constructed to hold the CTOD gage securely in position while allowing for ease of positioning as the crack extended. CTOD measurements were taken every 5 mm of crack extension or every 5000 cycles whichever came first. However, immediately following a tensile overload CTOD measurements were taken at 1, 10, 100, 500 and 1000 cycles. All CTOD measurements were taken during a complete loading cycle at 0.02 Hz.

The electrical analogs of CTOD and load were fed into a dual channel strip chart recorder which had a full scale deflection of 250 mm. Typical output readings are given in Figure 2. The load versus time curve is linear, but the CTOD versus time curve is non-linear. Crack closure and opening positions were taken from these curves at the beginning or ending of the linear CTOD versus time curves. Crack closure and opening loads were then determined from the corresponding load points. Due to difficulties in establishing the beginning of the non-linear region a reasonable scatter band of $\pm 444 \text{ N}$ existed for opening and closure loads. This resulted in a possible error up to ± 10 percent in opening stress levels, σ_{op} .

TEST RESULTS

Typical crack length versus applied cycles curves are shown in Figure 3 for both constant amplitude reference tests and single tensile overload tests for both $R = 0$ and $R = -1$ conditions. This figure represents a complete block of tests for 7075-T6 with $B = 6.3 \text{ mm}$. As found previously, the constant amplitude $R = 0$ and $R = -1$ data fall in a fairly narrow band for either 2024-T3 or 7075-T6 for negative R ratio not exceeding -1 [2, 3, 4, 7]. Also, as found previously with higher stress intensities, delay with $R = -1$ loading following a single tensile overload is less than for $R = 0$. The number of delay cycles, N_D , is labelled with a vertical arrow in Figure 3. Delay was defined essentially as the initial linear portion of the a versus N curve for a given overload. A complete summary of crack growth delay cycles, N_D is given in Table 1 for each overload test. This table shows that for a given material and thickness, the $R = -1$ loading following the single tensile overload caused reduced delay compared to the companion $R = 0$ test.

CTOD measurements for Figure 3 tests were converted to opening stress values, σ_{op} , and plotted as a function of a/W in Figure 4. σ_{op} was calculated from the opening load values as determined from data output represented in Figure 2. Substantial scatter existed in σ_{op} for a given loading with both constant amplitude reference tests and overload tests. This scatter was primarily due to the complexity of measuring CTOD and the location of the crack closure and opening values on the non-linear CTOD versus time curve. However, specific trends can be determined from the data. Curves for the other material and thicknesses were similar to Figure 4. Primary trends indicated that σ_{op} decreased for constant amplitude reference testing in a somewhat linear fashion and for a given a/W ,

σ_{op} was always higher for $R = 0$ than for $R = -1$. This difference is slight however when the scatter band is considered.

σ_{op} in the tensile overload tests always dropped below the initial reference test values just after the overload. Elber has predicted and noted this behaviour previously for primarily tensile loading [1]. However, this research indicates that similar initial drops occur for both $R = 0$ and $R = -1$ testing following a tensile overload. As additional cycles were applied to an overloaded specimen, σ_{op} increased during the delay period, reached a peak and then decreased in a manner similar to the constant amplitude reference behaviour. The influence of the tensile overload was essentially completed for both $R = 0$ and $R = -1$ when the peak value of σ_{op} was reached.

σ_{op} was converted to K_{op} using a linear curve fit equation with the following finite width stress intensity expression [8].

$$K = \frac{P\sqrt{a}}{BW} \left[1.99 - 0.41 \left\{ \frac{a}{W} \right\} + 18.7 \left\{ \frac{a}{W} \right\}^2 - 38.48 \left\{ \frac{a}{W} \right\}^3 + 53.85 \left\{ \frac{a}{W} \right\}^4 \right]$$

Representative values of K_{op} are plotted as the four lower curves in Figure 5 for 7075-T6 with $B = 6.3 \text{ mm}$. ΔK_{eff} was then determined from:

$$\Delta K_{eff} = K_{max} - K_{op}$$

Representative values of ΔK_{eff} are plotted on the four upper curves for 7075-T6 with $B = 6.3 \text{ mm}$ in Figure 5. ΔK_{eff} increased with applied cycles for both $R = 0$ and $R = -1$ constant amplitude testing, but often decreased slightly during the overload delay region and then increased. The point where delay terminated is located with a vertical arrow in Figure 5.

DISCUSSION OF RESULTS

The scatter in measuring σ_{op} and K_{op} of up to ± 10 percent of the maximum applied values places some limitations on the results of this research. However, substantial contributions are also made in that abrupt changes in measured σ_{op} and K_{op} occurred at conditions predicted by the crack closure model. These changes occurred just following the single tensile overload and as the crack grew out of the overload affected region. The magnitude of change however was not always in agreement with that found by Elber [1]. For example, σ_{op} in Figure 4 just following the overload reaches a minimum and then should increase and exceed the reference value preceding the overload. For all tests the increase occurred, but in most cases the maximum σ_{op} did not substantially exceed the pre-overload reference value. In Figure 4 substantial increases in σ_{op} occur following the overload for $R = -1$ but not for $R = 0$. In fact, the $R = -1$ maximum σ_{op} value exceeds that for $R = 0$. This behaviour is not consistent with delay data since $R = -1$ loading following an overload is detrimental relative to $R = 0$. Despite the somewhat disagreement in magnitude with Elber's work on overloads and crack closure, this research substantiates that crack closure exists and can be measured during negative R ratio cycling with and without tensile overloads. Thus a link between crack closure and retardation phenomena with both positive and negative R ratios exists. This is particularly seen in Figure 5 where increases in ΔK_{eff}

for $R = -1$ occur prior to increases in ΔK_{eff} for $R = 0$, which is in agreement with delay results.

Delay data in Table 1 indicate a definite overload thickness effect existed in both materials. For a given material and R ratio, N_D was greater with the thinner cross section. The crack closure model predicts that σ_{op} levels should decrease with increases in thickness if delay decreases with thickness. This difference, however, could not be ascertained in this research due to the substantial scatter.

Crack extension during the overload delay region was always less than about 0.25 mm for both R values. Thus, transients within the delay region could not be accurately measured. This 0.25 mm delay region is in complete agreement with the plane stress overload reversed plastic zones, RPZ, calculated from

$$RPZ = \frac{1}{4} \left[\frac{2}{2\pi} \left\{ k_{ol} / \sigma_Y \right\}^2 \right]$$

These plastic zones were approximately 0.4 mm for 2024-T3 and 0.2 mm for 7075-T6.

CONCLUSIONS

- 1) Crack closure was observed in both 2024-T3 and 7075-T6 aluminum while the SEN specimen was still in tension for both $R = 0$ and $R = -1$ constant amplitude and single tensile overload tests.
- 2) Crack closure predictions of delay following single tensile overloads agreed favourably with experimentally observed delay for both $R = 0$ and $R = -1$. This provides substantiation of the crack closure model.
- 3) Due to appreciable scatter σ_{op} levels following a tensile overload did not always exceed the magnitude of σ_{op} measured at similar crack lengths in $R = 0$ and $R = -1$ constant amplitude reference tests.
- 4) Delay following a single tensile overload was reduced by subsequent $R = -1$ loading compared to $R = 0$ loading. An increase in thickness also decreased delay following the tensile overload.
- 5) ΔK_{eff} values showed little difference for both $R = 0$ and $R = -1$ constant amplitude testing which is in agreement with similar crack growth data for $R = 0$ and $R = -1$.

REFERENCES

1. ELBER, W., "Damage Tolerance in Aircraft Structures", ASTM STP 486, 1971, 230.
2. STEPHENS, R. I., MCBURNEY, G. W. and OLIPHANT, L. J., International Journal of Fracture, 10, 1974, 587.
3. STEPHENS, R. I., CHEN, D. K. and HOM, B. W., "Fatigue Crack Growth Under Spectrum Loads", ASTM STP 595, 1976, 27.
4. STEPHENS, R. I., International Journal of Fracture, 12, 1976, 323.

5. STEPHENS, R. I., SHEETS, E. C. and NJUS, G. O., Symposium on Cyclic Stress-Strain and Plastic Deformation Aspects of Fatigue Crack Growth, St. Louis, Mo. U.S.A., May, 1976.
6. NJUS, G. O., Master of Science Thesis, The University of Iowa, July, 1976.
7. LANDGERUD, D. S. and STEPHENS, R. I., Second International Conference on Mechanical Behaviour of Materials, Boston, Mass., U.S.A., August, 1976.
8. BROWN, W. F. and SRAWLEY, J. E., "Plain Strain Crack Toughness Testing of High Strength Metallic Materials", ASTM STP 410, 1966, 12.

Table 1 Fatigue Crack Growth Delay Following Single Tensile Overload, OLR = 2.25, $K_{max i} = 12.3 \text{ MPa}\sqrt{\text{m}}$.

| | | 2024-T3 | 7075-T6 |
|---------|----|-----------------|-----------------|
| B mm | R | N_D cycles | N_D cycles |
| 3.15 | 0 | >250,000 | 50,000 |
| | -1 | 40,000 | 20,000 |
| 6.3 | 0 | 75,000 | 20,000 |
| | -1 | ----- | 12,500 |

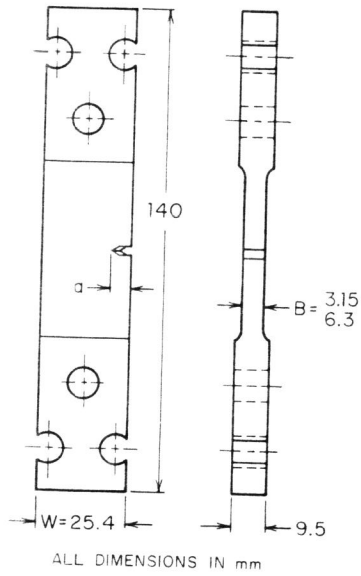


Figure 1 SEN Specimen

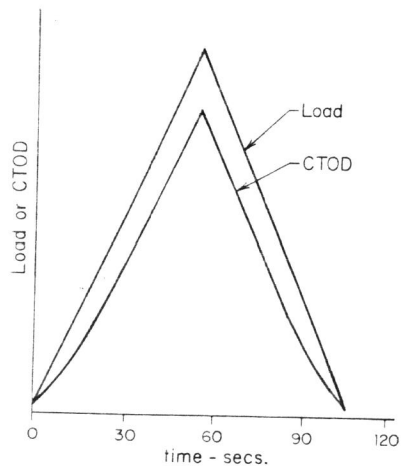


Figure 2 CTOD and Load Measurements, 7075-T6, B = 6.3 mm, R = 0, a = 9.6 mm

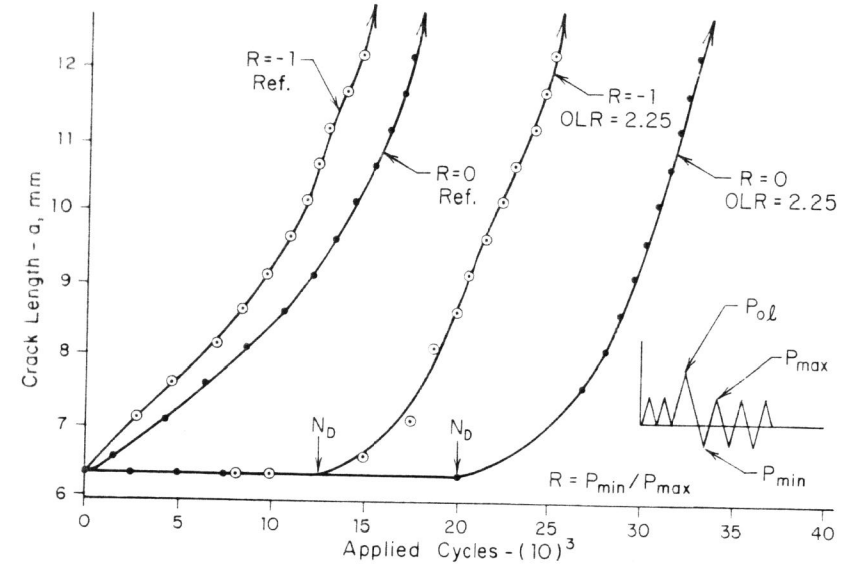


Figure 3 Fatigue Crack Growth Behavior, 7075-T6, B = 6.3 mm

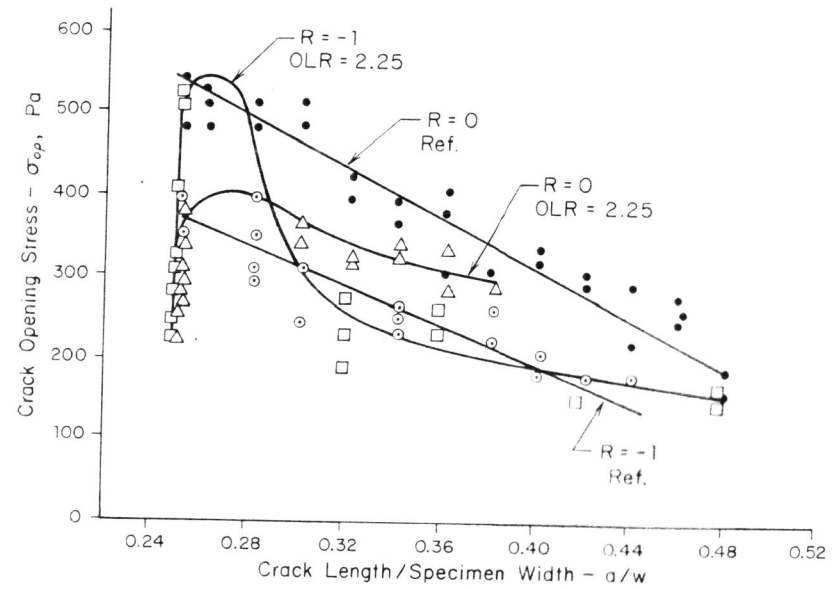


Figure 4 σ_{op} versus a/W 7075-T6, B = 6.3 mm

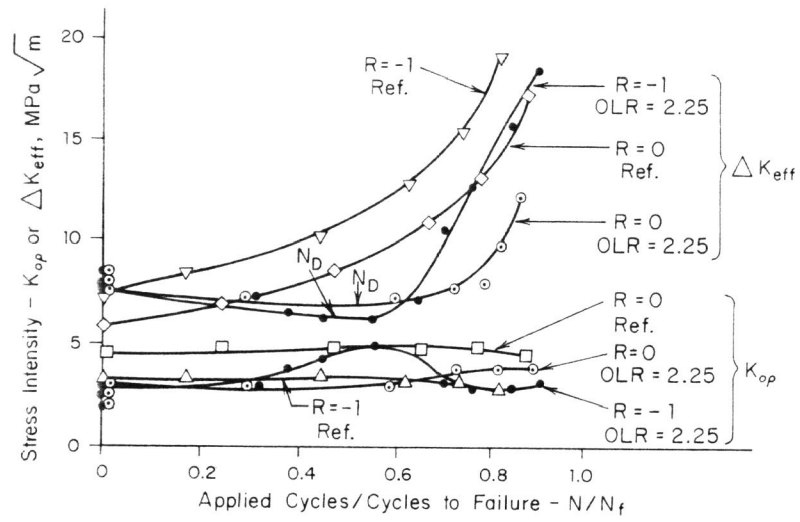


Figure 5 K_{op} and ΔK_{eff} versus N/N_f , 7075-T6, B = 6.3 mm